Epilepsy Research 178 (2021) 106808

Contents lists available at ScienceDirect

Epilepsy Research

journal homepage: www.elsevier.com/locate/epilepsyres

Mapping degeneration of the visual system in long-term follow-up after childhood hemispherectomy – A series of four cases

Luís Miguel Lacerda [a,*], Alki Liasis [b,c], Sian E. Handley [b], Martin Tisdall [d], J.Helen Cross [e], Faraneh Vargha-Khadem [e], Chris A. Clark [a]

[a] Developmental Imaging and Biophysics Section, UCL Great Ormond Street Institute of Child Health, London, United Kingdom
[b] Clinical and Academic Department of Ophthalmology, Great Ormond Street Hospital for Children NHS Foundation Trust and UCL Great Ormond Street Institute of Child Health, London, United Kingdom
[c] University of Pittsburgh Medical Centre, Children's Hospital of Pittsburgh, United Kingdom
[d] Neurosurgery, UCL Great Ormond Street Institute of Child Health, London, United Kingdom
[e] Clinical Neurosciences, UCL Great Ormond Street Institute of Child Health, London, United Kingdom

ARTICLE INFO

Keywords:
Hemidisconnection
Legacy
Tractography
Visual
Degeneration

ABSTRACT

Objective: Although hemidisconnection surgery may eliminate or reduce seizure activity in patients with epilepsy, there are visual, cognitive and motor deficits which affect patients' function post-operatively, with varying severity and according to pathology. Consequently, there is a need to map microstructural changes over long time periods and develop/apply methods that work with legacy data.
Methods: In this study, we applied the novel single shell 3-Tissue method to data from a cohort of 4 patients who were scanned 20-years following childhood hemidisconnection surgery and presented with variable clinical outcomes. We have successfully reconstructed tractography of the whole visual pathway from single shell diffusion data with reduced number of gradient directions.
Results: All patients presented with degeneration of the visual system characterised by low fractional anisotropy and high mean diffusivity. There were no apparent microstructural differences between both optic nerves that could explain the different level of visual function across patients. However, we provide evidence suggesting an association between the level of visual function and DTI metrics within the remaining components of the visual system, particularly the optic tract, of the contralateral hemisphere post-surgery.
Significance: We believe this study suggests that diffusion MRI can be used to monitor the integrity of the visual system following hemispherectomy and if extended to larger cohorts and a greater number of time-points, including pre-surgically, can provide a clearer picture of the natural history of visual system degeneration. This knowledge may in turn help to identify patients at greatest risk of poor visual outcomes that might benefit from rehabilitation therapies.

1. Introduction

Epilepsy is a medical condition in which the cells of the brain emit abnormal electrical activity resulting in seizures, which commonly lead to decline in brain function such as motor skills and cognition. Although the majority of patients with epilepsy can be managed with antiepileptic medication, for those with drug resistant epilepsy a remaining option is neurosurgical intervention.

Surgical intervention including local resection, lobectomy or in some cases hemispherectomy is possible if the epileptic focus can be isolated to one hemisphere. Hemispherectomy is characterised by disconnection of one of the hemispheres of the brain, which is structurally or functionally abnormal and causing seizures. Although this operation may eliminate or reduce seizure activity, there are visual, cognitive and motor deficits which have an effect on patient function post-operatively, with varying severity and according to pathology (Pulsifer et al., 2004; Werth, 2006). Therefore, the pre-surgical investigation and counselling of patients and their families is very important. Although these deficits are variable, among subjects, the motor deficits manifest as a hemiplegia contralateral to the resected hemisphere while cognitive outcomes are

* Correspondence to: Developmental Imaging and Biophysics Section, University College London Great Ormond Street Institute of Child Health, 30 Guilford Street, London WC1N 1EH, United Kingdom.
E-mail address: luis.lacerda@ucl.ac.uk (L.M. Lacerda).

https://doi.org/10.1016/j.eplepsyres.2021.106808
Received 3 June 2021; Received in revised form 18 October 2021; Accepted 2 November 2021
Available online 11 November 2021

Table 1
Summary of clinical data information. Sx – Surgery; M – Male; F- Female; RNFL – Retina Nerve Fibre Layer.

Patient number	Sex	Side of surgery	Aetiology	Functional or anatomical surgery	Age at Sx (years)	Follow up time (years)	Age at assessment (years)	Global RNFL of the contralateral eye (μm)	Global RNFL of the ipsilateral eye (μm)	Visual acuity in contralateral eye (logMar)	Visual acuity in ipsilateral eye (logMar)
1	M	Left	Middle cerebral artery infarct and left sided atrophy	Functional	15.1	6.4	21.5	82	90	-0.040	-0.040
2	M	Right	Right hemimegancephaly	Anatomical	4.2	19.4	23.6	81.3	101.4	0.440	0.040
3	M	Left	Left Sturge-Weber	Anatomical	8.5	25.0	33.5	69	86	0.400	0.100
4	F	Left	Small left hemisphere possible pre/perinatal stroke	Functional	2.3	28.8	31.1	45	50	0.700	0.060

aetiology dependent (Moosa et al., 2013). In particular for the visual system, whilst all patients will have a homonymous hemianopia post-operatively it is important to recognise, that in some cases, the visual field deficit is already present pre-operatively. As a consequence of having hemisphere dysfunction, a specific pattern of trans-synaptic degeneration (TSRD) can be observed within the eyes (Hoyt et al., 1972; Jindahra et al., 2012). Although the effects of TSRD have long been observed (Buren, 1963) they have recently been further investigated with more objective measures such as optical coherence tomography (OCT) (de Vries-Knoppert et al., 2019).

A recent investigation of visual function in six adults 20 years after they underwent hemispherectomy in childhood for intractable epilepsy (Handley et al., 2017) revealed an intraocular difference with the eye ipsilateral to the side of the hemispherectomy having better visual function and thicker retinal nerve fibre layer (RNFL) than the contralateral eye. The better function in the ipsilateral eye was consistently evident in both objective tests: pattern visual evoked potential (VEP) and OCT measures of the RNFL, plus subjective visual acuity (VA) and kinetic visual field. Within the cohort there was also a range of visual impairment observed in the visual field from the remaining hemisphere that was unexpected and unexplained.

In the above cohort, magnetic resonance imaging (MRI) data was collected but not analysed. Analysis of this data would aid the investigation of structural changes in the visual pathways beyond the behavioural and electrophysiological methods, that may shed light on the inter ocular difference in function observed and the range of visual dysfunction in the remaining field. In particular, diffusion tensor imaging (DTI) (Basser et al., 1994) is a technique sensitive to the motion of water molecules which provides a way to probe tissue microstructure and the architecture of white matter pathways in vivo and non-invasively, the latter through a technique called tractography. DTI and tractography have been used to perform reconstructions of the human visual pathways (Hofer, 2010), for pre-surgical planning (Winston et al., 2014), in intraoperative settings (Daga et al., 2012) and to understand varied patterns of degeneration following surgery (Millington et al., 2014). Nonetheless, DTI lacks specificity in regions of very complex microstructural arrangements (Alexander et al., 2007) and it is thus less suitable to provide artefact free reconstructions of white matter pathways in those cases (Farquharson et al., 2013). Recent advances in both scanning and modelling technologies have however enabled the development of more advanced diffusion MRI models which move beyond the limitations of DTI (Jeurissen et al., 2014; Tournier et al., 2012) and these have already been successfully used to assess visual outcomes in pathological conditions and following surgery (Hales et al., 2018; Lacerda et al., 2020). The challenge remains to apply these techniques to legacy data which remain extremely important to shed further light into the mechanisms of degeneration of the visual system following surgery.

Therefore, in this study we have applied a novel algorithm (Dhollander & Connelly, 2016) that has been designed to extract more detailed information about diffusion within white matter from a limited set of data, originating from a study of long-term outcomes following hemidisconnection surgery for epilepsy in childhood. Most importantly, we set out to further understand why in the long term some patients had unexpectedly much better residual visual function in the eye ipsilateral to the resection, and why some participants had significant constriction of the remaining visual field. The information about predicted post-operative visual function is of utmost importance as it consists of a very important aspect of pre-operative counselling and the decision for the family to proceed with surgery.

2. Materials and methods

The study was an observational case series and approved by the National Health Service Research Ethics Committee for London – City Road & Hampstead and followed the tenets of the Declaration of Helsinki. In brief, of the original 6 patients first analysed in (Handley et al., 2017) two patients were excluded, one for not having MRI data (due to a metal clip in situ preventing scanning) and another due to excessive motion artefacts, which rendered the data unusable for analysis. The remaining four patients had a mean age of 27.4 years at scan, average time since surgery was 19.9 years and three out of four had left sided hemispherectomies (and right homonymous hemianopia) – a summary of the full clinical details, including relevant ophthalmological findings from (Handley et al., 2017) can be found in Table 1. Patient 1 was noted to have weakness of the right side of the body at 9 months after birth. Seizures began at the age of 12 years. An MRI scan was conducted and he was found to have a mature lesion of the left hemisphere due to middle cerebral artery infarction and left sided atrophy. Patient 2 had hemimegalencephaly, which is a rare condition where one hemisphere of the brain is larger than the other, with an affected right hemisphere and weakness of the left side of the body noted at 8 months of age. Patient 3 was born with a left facial port wine stain, and CT of the brain revealed corresponding left hemiatrophy. He was diagnosed with Sturge-Weber syndrome which is a condition that affects the development of certain blood vessels, causing abnormalities in the brain, skin, and eyes from birth. His first seizure was at 6 days of life (Vargha-Khadem, 1997). Finally, patient 4 revealed weakness of the right side of the body at 6 months after birth. Seizures began at the age of 7 years. A CT scan performed at diagnosis showed marked left hemi-atrophy with almost all of the cortical mantle destroyed, except for a small remnant in the frontal region. The removed hemisphere underwent neuropathological examination and appearances suggested circulatory damage had occurred in the perinatal period.

Analysis of the MRI scans was undertaken in a semi-blinded fashion. The scans were anonymised and the person undertaking the analysis (LML) whilst aware of side of surgery (and therefore resulting side of field defect), was not aware of the further details of the ophthalmic findings of each individual patient (Handley et al., 2017). MRI (standard brain and pituitary scan) and DTI sequences were acquired on an Avanto 1.5 Tesla scanner (Siemens, Erlangen, Germany). Echo-planar diffusion

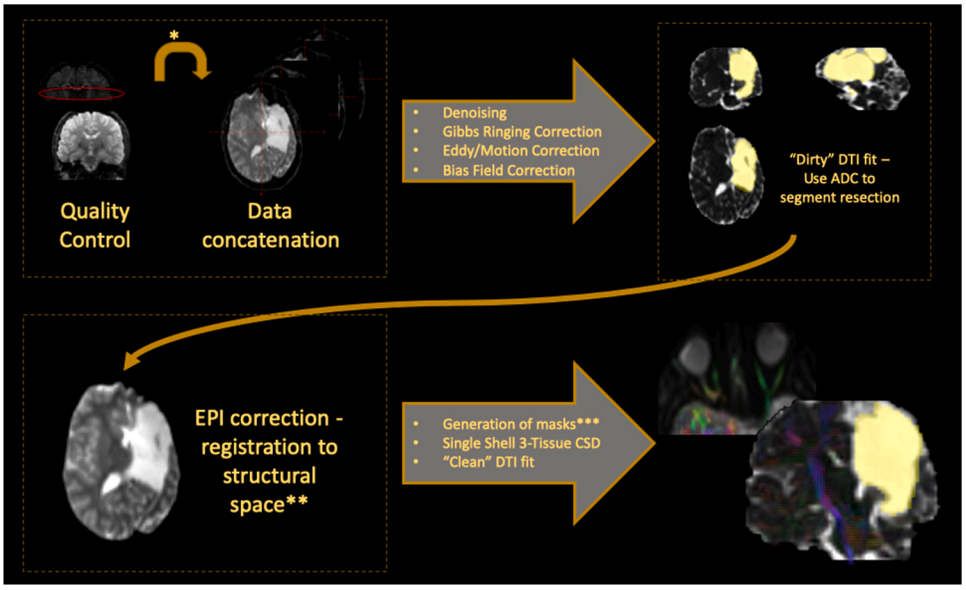

Fig. 1. Overview of processing pipeline: * Number of slices had to be matched before concatenation of different diffusion datasets; ** Field of view of structural scan adapted to match diffusion data prior to registration/ diffusion directions (bvec) reoriented with affine matrix resulting from registration procedure *** Developed semi-automatic procedure to segment the eyes from b0 images (supplementary material) – this was then merged with the average b0 and manually edited to cover the region of the optic nerves.

weighted images were acquired for an isotropic set of 20 non-collinear directions, using a weighting factor of b = 1000 s.mm^{-2}, along with a T2-weighted (b0) volume. This protocol was repeated three times in a single scan session, including 45 contiguous axial slices of thickness 2.5 mm per dataset, using a field of view of 240 × 240 mm and 96 × 96 voxel acquisition matrix, for a final image resolution of 2.5 × 2.5 × 2.5 mm. Echo time was 89 ms and repetition time was 6300 ms. In addition, an identical protocol with 60 non-collinear gradient directions and three b0 volumes was acquired. Finally, a T1-weighted 3D FLASH structural image was acquired using 176 contiguous sagittal slices, a 256 × 224 mm field of view, a flip angle of 15 degrees and 1 × 1 × 1 mm image resolution. Echo time in this case was 4.9 ms, and repetition time was 11 ms.

2.1. Quality control and pre-processing

The first step was to visually assess all datasets and discard corrupted volumes before concatenating all multiple diffusion acquisitions – this was done to increase SNR and the angular coverage as provided by different diffusion directions (the complete image analysis pipeline is shown in Fig. 1). Pre-processing was then initiated with denoising (Veraart et al., 2016), Gibbs ringing correction and eddy current and motion distortion correction using MRtrix3 (Tournier et al., 2019) and FSL tools (Jenkinson et al., 2012). Since there was no available data to model the susceptibility distortions and correct them using state of the art tools, we applied EPI distortion correction by registering the average b0 scan to the structural scan with the Advanced Normalisation Tools Software (ANTs) (Avants et al., 2014). In order to prevent the resection area driving the registration we reconstructed a first estimation of the diffusion tensor for the concatenated dataset, segmented the resected area on the mean diffusivity (MD) map, and used its inverse as a mask in the registration procedure (so that the resection could be ignored). After EPI correction we then applied the recently developed single shell 3-Tissue constrained spherical deconvolution to extract fibre orientation distribution functions for our data using the MRtrix3Tissue tool (https://3Tissue.github.io). It is worth mentioning that this method was developed to make use of legacy data (where traditionally only single shell and lower b value diffusion weighted data is available). The individual diffusion datasets that were concatenated before pre-processing were then split back according to the original distribution (as described in the methods section above) and the DTI model was applied once again for each corrected dataset - MD and fractional anisotropy (FA) metrics were computed.

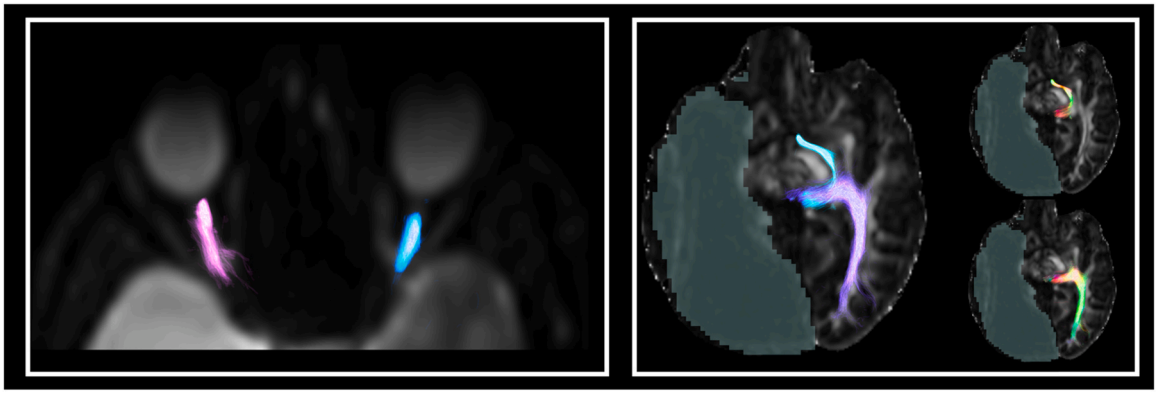

Fig. 2. Reconstruction of the full visual pathways highlighting probability of anatomical connections for the optic nerves (left) and post-chiasmal structures – optic tract and optic radiation (right). A random solid colour was chosen to represent each structure – both optic nerves and contralateral optic tract and optic radiation. In addition, two smaller figures display the traditional directional colour encoding in diffusion imaging (Red: left-right; Green: anterior-posterior; Blue: inferior-superior).

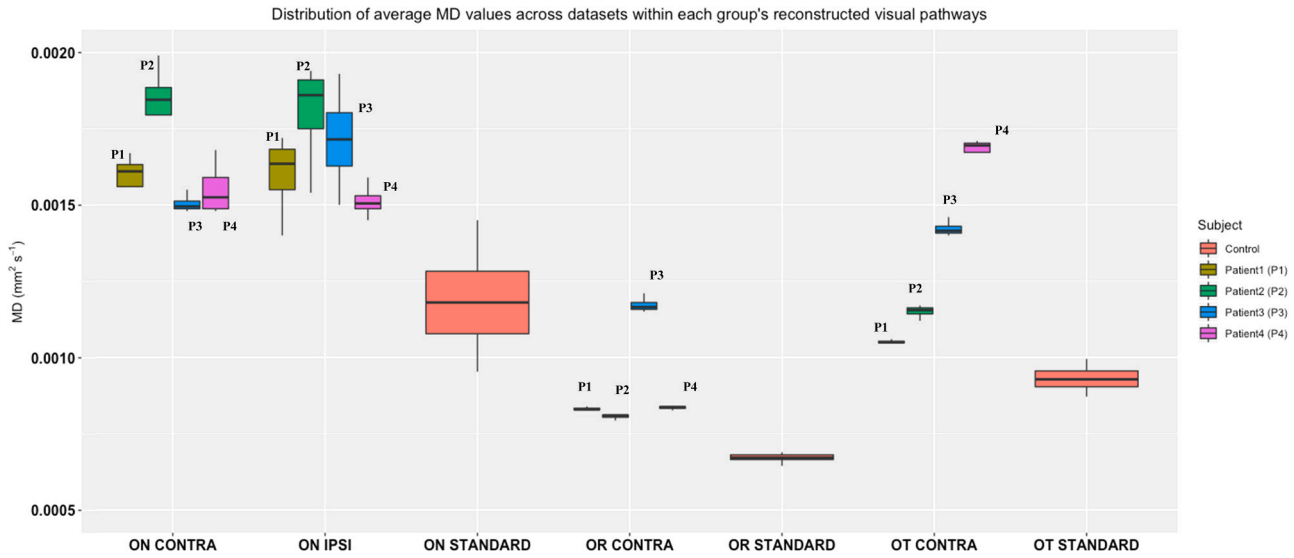

Fig. 3. Average mean diffusivity (MD) within the ipsi and contra lateral optic nerve (ON) as well as contra-lateral optic radiation (OR) and optic tract (OT) for the four patients for which data was available. Each patient's boxplot is showing the variability in the average MD values extracted for each dataset available per subject group, i.e; for the control group it is showing the variability across twenty different identical datasets and for each patient it is showing the variability across the four datasets described in the methods. The boxplot visualises five summary statistics (the median, two hinges and two whiskers), and all "outlying" points individually, which are beyond 1.5* inter quartile range (IQR) of either the lower or higher whisker.

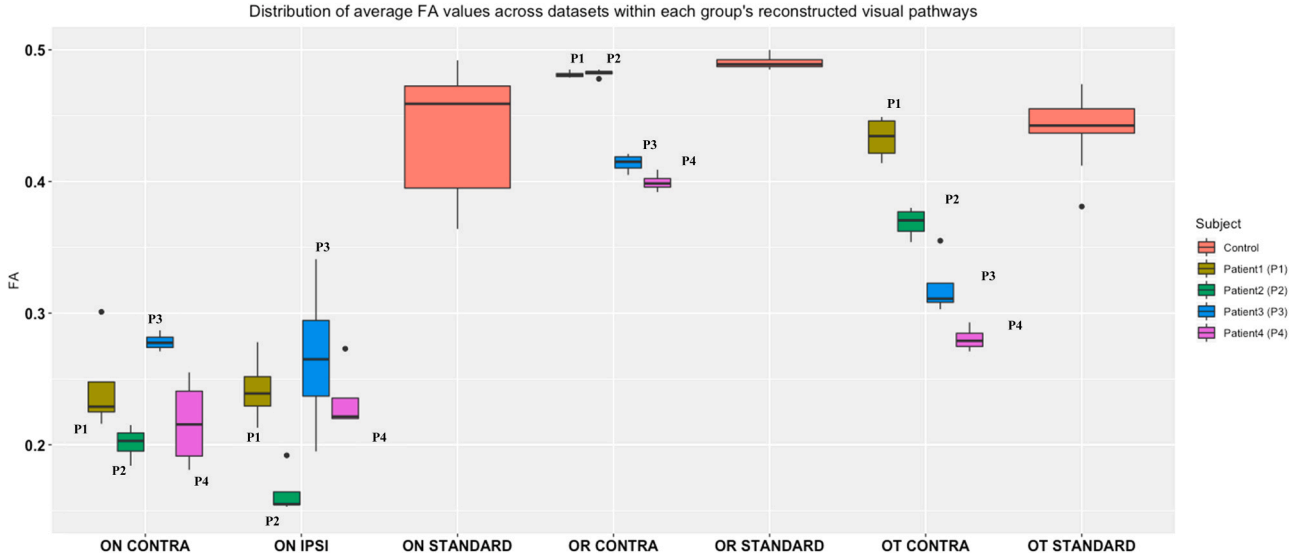

Fig. 4. Average fractional anisotropy (FA) within the ipsi and contra lateral optic nerve (ON) as well as contra-lateral optic radiation (OR) and optic tract (OT) for the four subjects for which data was available. Each patient's boxplot is showing the variability in the average FA values extracted for each dataset available per subject group, i.e; for the control group it is showing the variability across twenty different identical datasets and for each patient it is showing the variability across the four datasets described in the methods. The boxplot visualises five summary statistics (the median, two hinges and two whiskers), and all "outlying" points individually, which are beyond 1.5* inter quartile range (IQR) of either the lower or higher whisker.

2.2. Tractography and clinic-anatomical relationships

We derived reconstructions of the complete visual pathways, including both optic nerves (ON), contralateral optic tract (OT) and optic radiation (OR). Regarding the optic nerves, in each slice where the optic nerve could be identified, an experienced clinical scientist (AL) placed regions of interest (ROI), which were used to seed tractography. This was done in an iterative manner until the optic nerves were isolated. We also used ROIs to exclude the contribution of the muscles of the eyes. The termination of the optic nerve (optic chiasm) was then used as a seed region for the optic tract tractography with a target region being selected at the level of the lateral geniculate nucleus (LGN). For the optic radiation we followed the procedure described in a previous paper (Lacerda et al., 2020). Fig. 2 shows a reconstruction of the full visual pathways for one of the patients in this cohort. Following the reconstruction of the relevant structures of interest, we computed probability of connection maps of the different structures - ON, OR and OT – and extracted a weighted mean for each DTI parameter within those maps (Figs. 3 and 4). Finally, to evaluate any relationship that could explain the inter-ocular difference observed in (Handley et al., 2017) we plotted ophthalmological values of RNFL and VA of both eyes with the metrics extracted for each reconstructed structure of the visual pathways.

Although the main focus of this study was the four cases described

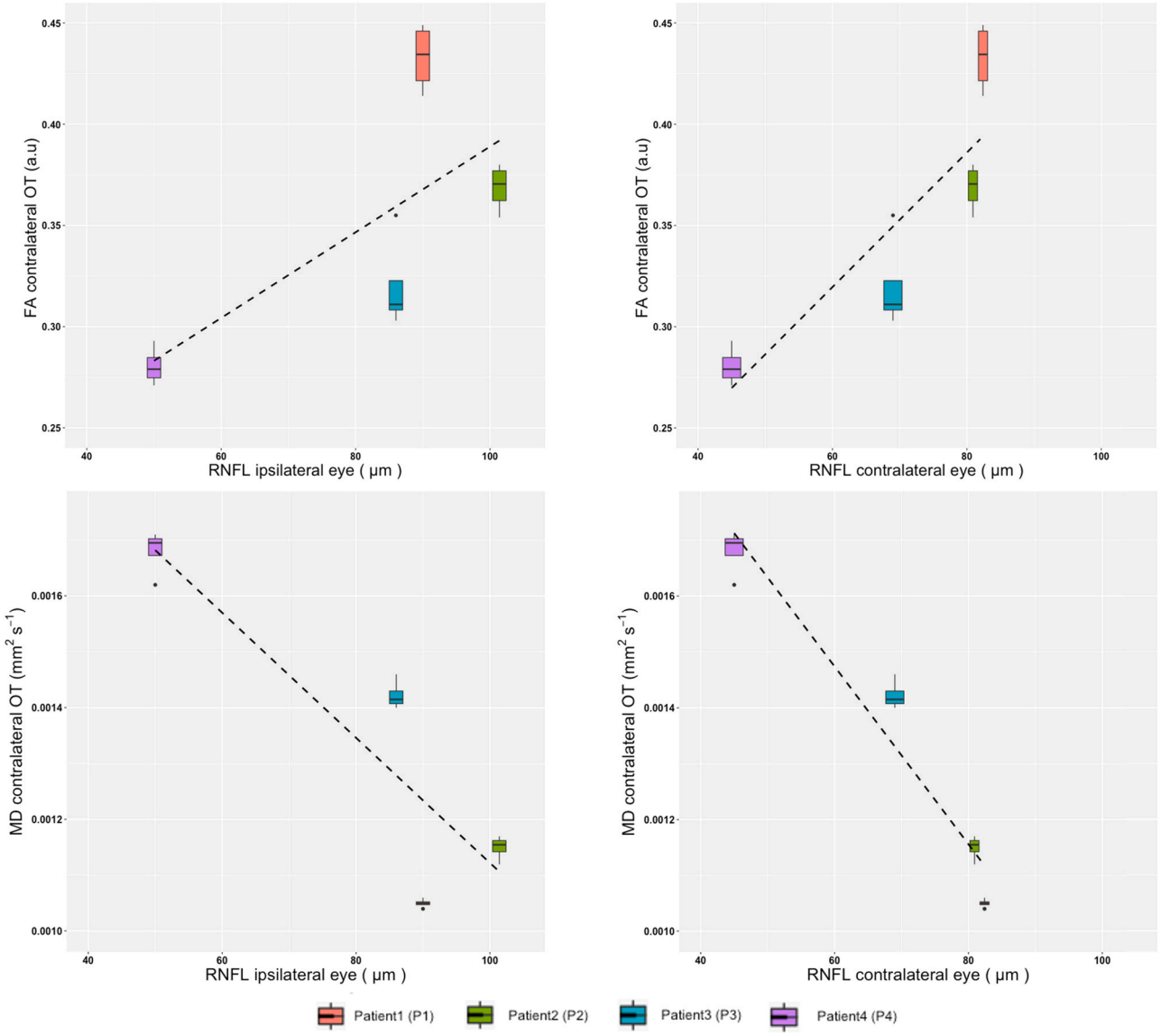

Fig. 5. Relationship of FA and MD in the contralateral optic tract and Retina Nerve Fibre Layer (RNFL) for both ipsi and contralateral Eyes.

above, we have also reconstructed metrics of interest in a group of 20 age-matched healthy controls (median age of 31.35 years, inter-quartile range 7.4 years; 3 male) purely to provide a visual reference. Qualitatively we can appreciate that for all patients and all components of the visual system (ON, OR and OT) there are abnormalities characterised by increases in mean diffusivity and reductions in fractional anisotropy (Figs. 3 and 4). In all patients, both MD and FA are very similar between the ipsi- and contralateral optic nerves. However, analysis of the remaining structures in the contralateral hemisphere showed differences in FA and MD across patients. Out of all the plots exploring the reconstructed imaging metrics against the original visual data presented in Table 1, we highlight those between MD and FA in the contralateral optic tract with the values of remaining visual function measured by RNFL (µm) and VA (logMAR) (Figs. 5 and 6). Finally, reconstructed values within the optic radiation and optic tract were more reproducible across the available diffusion datasets whereas the optic nerves showed higher variability.

3. Discussion

In this study, we have successfully reconstructed the complete visual pathways of four adults who underwent hemispherectomy in childhood, employing a recently developed methodology (Dhollander & Connelly, 2016) which allows estimating measures of fibre orientations from single shell diffusion MRI data.

3.1. Abnormal structure of the optic nerves as result of trans-synaptic retrograde degeneration

Our study adds further to the evidence that trans-synaptic retrograde degeneration of the visual system does take place in the brain (Ptito et al., 2001) as highlighted by abnormal diffusion metrics in the optic nerves of all four patients with hemidisconnection assessed in long-term follow-up. However, diffusion imaging did not reveal any structural differences between the optic nerves that could explain the inter ocular differences found in the ophthalmological parameters (RNFL and VA). Although the result of unilateral cortical lesions on the integrity of the optic nerves is still not clearly understood, we suspect that the inter ocular difference of ophthalmic measures reported in the previous study (Handley et al., 2017) can potentially be explained by the difference in distribution of the nasal and temporal field ganglion cells entering the optic nerve and their susceptibility to TRSD. It is currently not

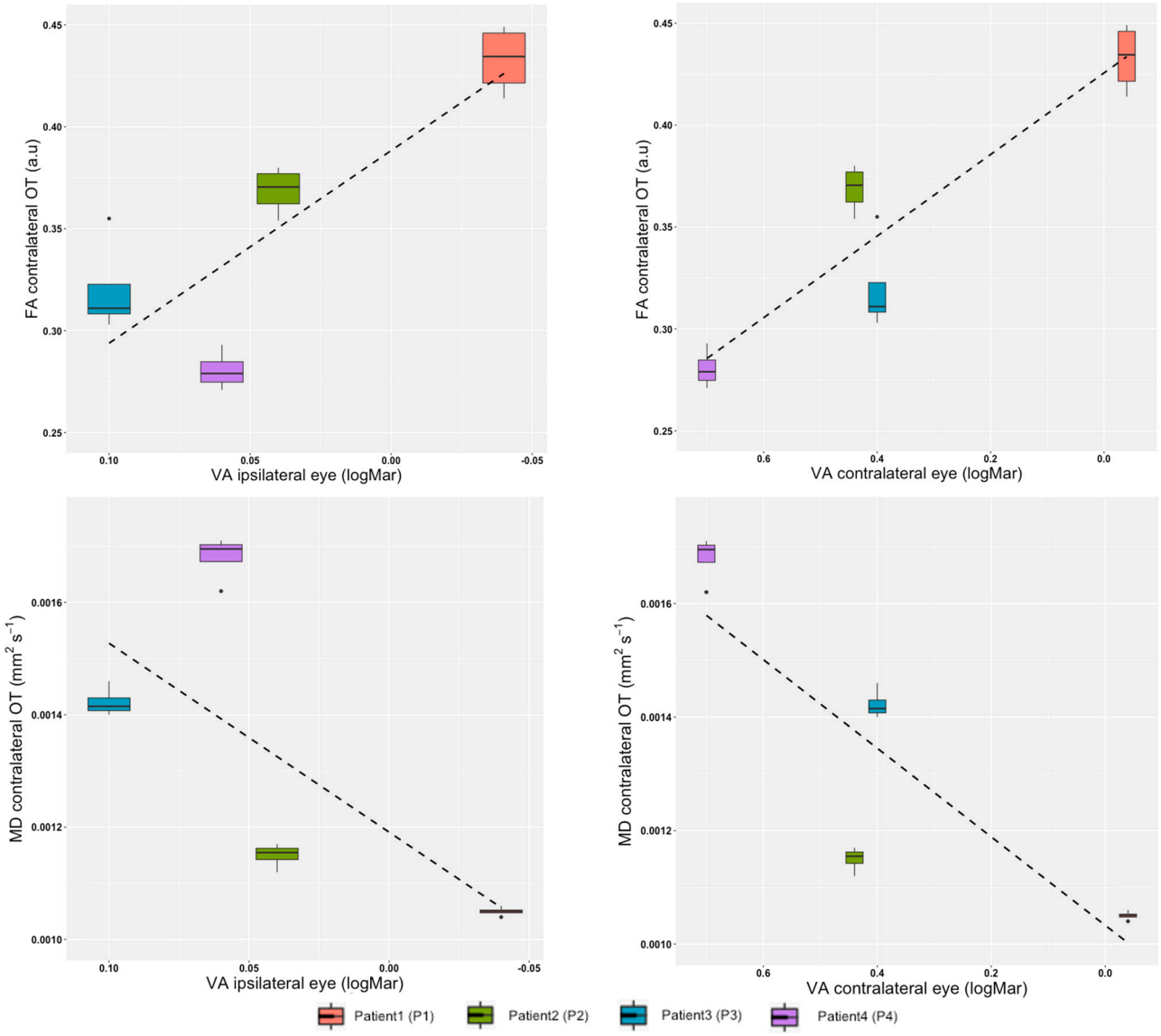

Fig. 6. Relationship of FA and MD in the contralateral optic tract and Visual Acuity (VA) for both ipsi and contralateral Eyes.

methodologically possible to evaluate this difference, and therefore further work on obtaining high-resolution imaging of the optic nerves would be valuable to dissect the crossing and non-crossing fibre distributions within the optic nerve (Fraser et al., 2011) and determine their relative distribution in subserving both temporal and nasal fields in each eye.

3.2. *Considerations on pre-surgical brain abnormalities and post-surgical visual function*

To provide an accurate representation of the remaining visual function following surgery it is not only important to address the direct effect of surgically disconnecting one hemisphere, but also the ability of the remaining hemisphere to support vision. Although the detected abnormalities in the affected (and consequently operated) hemisphere are generally higher when compared to contralateral hemisphere (Hallbook et al., 2010), the integrity of the remaining hemisphere is important to predict clinical outcomes (Mehta & Plant, 2005; Traub--Weidinger et al., 2016; Bridge et al., 2011; Jindahra et al., 2012; Rispoli et al., 2019). In fact, our results suggest that there is an association between the extent of damage in the contralateral optic tract (altered MD and FA metrics) and the lowest level of visual function in every patient as measured by OCT and logMAR scores (Figs. 5 and 6) – viz, patient 1 with best vision has the highest FA and lowest MD, whereas patient 4 with the poorest vision has the opposite. Although it is expected that the follow-up time after surgery is related to the level of degeneration (see Table 1), the fact that we don't find a similar association with the optic radiations warrants further investigation. Not only it will be imperative to evaluate pre-surgical measures of RNFL and integrity of the visual system (not available for this study) but also to investigate other clinical variables such (e.g age at surgery, aetiology of the disease) and age/gender effects which can reveal more specific details of the degeneration taking place.

3.3. *Limitations*

Working with legacy datasets is unavoidable and incurs technical difficulties, in particular whilst reconstructing structures as challenging as the optic nerves (Roebroeck et al., 2008; Jacquesson et al., 2019).

Without specific methods to account for eye-movements (Sengupta et al., 2017) and acquisition related distortions (Smith et al., 2011) there can be unaccounted changes in the optic nerve conformation (Lee et al.,

2018); furthermore, without a reduced field of view and increased resolution (Trip et al., 2006) these acquisitions are more susceptible to partial volume effects - these have probably affected our reconstructed metrics (particularly high MD in the optic nerves) despite a very low variability across datasets (Sarlls & Pierpaoli, 2009). Substantial differences in FA in visual system structures as compared to controls can be appreciated visually in Fig. 4. We recognise that due to differences in signal to noise ratio between 1.5 T and 3 T this can cause a systematic bias in FA (Alexander et al., 2006; Grech-Sollars et al., 2015). However, these biases are small when compared to the magnitude of FA changes that we observe in these patients at long follow-up times following hemidisconnection surgery.

Notwithstanding the limited sample, with a range of underlying pathologies for each patient it is important to highlight that this is one of the first studies that shows the feasibility of using the single shell 3-tissue spherical deconvolution technique with legacy data, allowing the mapping of grey matter, cerebrospinal fluid and white matter compartments to improve reconstruction of fibre directionality in the brain (Khan et al., 2020). Despite having a lower angular contrast provided by fewer directions than current state of the art acquisitions, even highly angulated structures such as Meyer's loop could be accurately reconstructed using these methods, which opens good opportunities to further explore historical datasets and aid the characterisation of long-term degeneration following surgery.

3.4. Future questions and applications

The development of imaging metrics that help predict visual function after surgery may play an important role in advising families before a surgical decision is made – in particular in (McGovern et al., 2019), atrophy in cerebral peduncles prior to surgery is indicative of better postoperative motor function. Similarly to visual function (P. Jindahra et al., 2009), our findings can help shed light on the efficacy of future interventions as well as aid further comprehension of patterns and timing of trans synaptic degeneration. Furthermore, it has been postulated that the potential for neuroplasticity is maximal when the operation is performed early in life, but there are some cases that show this can also be possible in adulthood (Damasio et al., 1975). The determinants of plasticity are, however, still not fully identified and it will be important to consider them in light of the age at surgery and onset of epilepsy, type of pre-existing deficits and abnormal development (Muckli et al., 2009) as well as the de facto establishment of new connections following surgery (Holloway, 2000). A future longitudinal study would be able to answer some of these questions, as well as providing a careful evaluation of changes in the brain as a result of visual rehabilitation techniques (Ong et al., 2012; Waddington et al., 2018).

4. Conclusion

This study demonstrates microstructural damage to the optic nerves, optic tracts and optic radiations at long-term follow-up in patients undergoing hemispherectomy for intractable epilepsy in childhood. In this small selected cohort it was observed that diffusion metrics, particularly in the optic tracts, mirrored the retinal nerve fibre layer and visual acuity indices, indicating that greater microstructural damage or its location was associated with poorer visual outcome. This study suggests that diffusion MRI can be used to monitor the integrity of the visual system following hemispherectomy and if extended to larger cohorts and a greater number of time-points, including pre-surgically, can provide a clearer picture of the natural history of visual system degeneration. This knowledge may in turn help to identify those patients at greatest risk of poor visual outcomes that can benefit from rehabilitation therapies.

Disclosure

The authors have no conflicts of interest to disclose. Furthermore, we confirm that we have read the Journal position on issues involved in ethical publication and affirm that this report is consistent with those guidelines.

Acknowledgements

This research was supported by the NIHR Great Ormond Street Hospital Biomedical Research Centre. The views expressed are those of the author(s) and not necessarily those of the NHS, the NIHR or the Department of Health. LML acknowledges that all co-authors have been substantially involved in the study and/or the preparation of the manuscript and have seen and approved the submitted version of the paper, accepting responsibility for its content.

References

Alexander, A.L., Lee, J.E., Lazar, M., Field, A.S., 2007. Diffusion tensor imaging of the brain. Neurotherapeutics 4 (3), 316–329. https://doi.org/10.1016/j.nurt.2007.05.011.

Alexander, A.L., Lee, J.E., Wu, Y.-C., Field, A.S., 2006. Comparison of Diffusion Tensor Imaging Measurements at 3.0 T versus 1.5 T with and without Parallel Imaging. Neuroimaging Clin. 16 (2), 299–309. https://doi.org/10.1016/j.nic.2006.02.006.

Avants, B.B., Tustison, N.J., Stauffer, M., Song, G., Wu, B., Gee, J.C., 2014. The Insight ToolKit image registration framework. Front. Neuroinf. 8, 8. https://doi.org/10.3389/fninf.2014.00044.

Basser, P.J., Mattiello, J., LeBihan, D., 1994. MR diffusion tensor spectroscopy and imaging. Biophys. J. 66 (1), 259–267. https://doi.org/10.1016/S0006-3495(94)80775-1.

Bridge, H., Jindahra, P., Barbur, J., Plant, G.T., 2011. Imaging Reveals Optic Tract Degeneration in Hemianopia. Investig. Opthalmol. Visual Sci. 52 (1), 382–388. https://doi.org/10.1167/iovs.10-5708.

Buren, J.M.V., 1963. Trans-synaptic retrograde degeneration in the visual system of primates. J. Neurol., Neurosurg. Psychiatry 26 (5), 402–409. https://doi.org/10.1136/jnnp.26.5.402.

Daga, P., Winston, G., Modat, M., White, M., Mancini, L., Cardoso, M.J., Symms, M., Stretton, J., McEvoy, A.W., Thornton, J., Micallef, C., Yousry, T., Hawkes, D.J., Duncan, J.S., Ourselin, S., 2012. Accurate localization of optic radiation during neurosurgery in an interventional MRI suite. IEEE Trans. Med. Imag. 31 (4), 882–891. https://doi.org/10.1109/TMI.2011.2179668.

Damasio, A.R., Lima, A., Damasio, H., 1975. Nervous function after right hemispherectomy. Neurology 25 (1), 89. https://doi.org/10.1212/WNL.25.1.89.

de Vries-Knoppert, W.A., Baaijen, J.C., Petzold, A., 2019. Patterns of retrograde axonal degeneration in the visual system. Brain 142 (9), 2775–2786. https://doi.org/10.1093/brain/awz221.

Dhollander, T., Connelly, A., 2016. A novel iterative approach to reap the benefits of multi-tissue CSD from just single-shell (+b=0) diffusion MRI data. Int. Soc. Magn. Resonance Med.

Farquharson, S., Tournier, J.-D., Calamante, F., Fabinyi, G., Schneider-Kolsky, M., Jackson, G.D., Connelly, A., 2013. White matter fiber tractography: why we need to move beyond DTI. J. Neurosurg. 118 (6), 1367–1377. https://doi.org/10.3171/2013.2.JNS121294.

Fraser, J.A., Newman, N.J., Biousse, V., 2011. Disorders of the optic tract, radiation, and occipital lobe. Handb. Clin. Neurol. 205–221. https://doi.org/10.1016/B978-0-444-52903-9.00014-5.

Grech-Sollars, M., Hales, P.W., Miyazaki, K., Raschke, F., Rodriguez, D., Wilson, M., Gill, S.K., Banks, T., Saunders, D.E., Clayden, J.D., Gwilliam, M.N., Barrick, T.R., Morgan, P.S., Davies, N.P., Rossiter, J., Auer, D.P., Grundy, R., Leach, M.O., Howe, F. A., Clark, C.A., 2015. Multi-centre reproducibility of diffusion MRI parameters for clinical sequences in the brain. NMR Biomed. 28 (4), 468–485. https://doi.org/10.1002/nbm.3269.

Hales, P.W., Smith, V., Dhanoa-Hayre, D., O'Hare, P., Mankad, K., D'Arco, F., Cooper, J., Kaur, R., Phipps, K., Bowman, R., Hargrave, D., Clark, C., 2018. Delineation of the visual pathway in paediatric optic pathway glioma patients using probabilistic tractography, and correlations with visual acuity. NeuroImage: Clin. 17, 541–548. https://doi.org/10.1016/j.nicl.2017.10.010.

Hallbook, T., Ruggieri, P., Adina, C., Lachhwani, D.K., Gupta, A., Kotagal, P., Bingaman, W.E., Wyllie, E., 2010. Contralateral MRI abnormalities in candidates for hemispherectomy for refractory epilepsy. Epilepsia 51 (4), 556–563. https://doi.org/10.1111/j.1528-1167.2009.02335.x.

Handley, S.E., Vargha-Khadem, F., Bowman, R.J., Liasis, A., 2017. Visual function 20 years after childhood hemispherectomy for intractable epilepsy. Am. J. Ophthalmol. 177, 81–89. https://doi.org/10.1016/j.ajo.2017.02.014.

Hofer, S., 2010. Reconstruction and dissection of the entire human visual pathway using diffusion tensor MRI. Front. Neuroanatomy. https://doi.org/10.3389/fnana.2010.00015.

Holloway, V., 2000. The reorganization of sensorimotor function in children after hemispherectomy: A functional MRI and somatosensory evoked potential study. Brain 123 (12), 2432–2444. https://doi.org/10.1093/brain/123.12.2432.

Hoyt, W.F., Rios-Montenegro, E.N., Behrens, M.M., Eckelhoff, R.J., 1972. Homonymous hemioptic hypoplasia. Fundoscopic features in standard and red-free illumination in three patients with congenital hemiplegia. Br. J. Ophthalmol. 56 (7), 537–545. https://doi.org/10.1136/bjo.56.7.537.

Jacquesson, T., Frindel, C., Kocevar, G., Berhouma, M., Jouanneau, E., Attyé, A., Cotton, F., 2019. Overcoming challenges of cranial nerve tractography: a targeted review. Neurosurgery 84 (2), 313–325. https://doi.org/10.1093/neuros/nyy229.

Jenkinson, M., Beckmann, C.F., Behrens, T.E.J., Woolrich, M.W., Smith, S.M., 2012. FSL. NeuroImage 62 (2), 782–790. https://doi.org/10.1016/j.neuroimage.2011.09.015.

Jeurissen, B., Tournier, J.-D., Dhollander, T., Connelly, A., Sijbers, J., 2014. Multi-tissue constrained spherical deconvolution for improved analysis of multi-shell diffusion MRI data. NeuroImage 103, 411–426. https://doi.org/10.1016/j.neuroimage.2014.07.061.

Jindahra, P., Petrie, A., Plant, G.T., 2009. Retrograde trans-synaptic retinal ganglion cell loss identified by optical coherence tomography. Brain 132 (3), 628–634. https://doi.org/10.1093/brain/awp001.

Jindahra, P., Petrie, A., Plant, G.T., 2012. The time course of retrograde trans-synaptic degeneration following occipital lobe damage in humans. Brain 135 (2), 534–541. https://doi.org/10.1093/brain/awr324.

Khan, W., Egorova, N., Khlif, M.S., Mito, R., Dhollander, T., Brodtmann, A., 2020. Three-tissue compositional analysis reveals in-vivo microstructural heterogeneity of white matter hyperintensities following stroke. NeuroImage 218, 116869. https://doi.org/10.1016/j.neuroimage.2020.116869.

Lacerda, L.M., Clayden, J.D., Handley, S.E., Winston, G.P., Kaden, E., Tisdall, M., Cross, J.H., Liasis, A., Clark, C.A., 2020. Microstructural investigations of the visual pathways in pediatric epilepsy neurosurgery: insights from multi-shell diffusion magnetic resonance imaging. Front. Neurosci. 14 https://doi.org/10.3389/fnins.2020.00269.

Lee, W.J., Kim, Y.J., Kim, J.H., Hwang, S., Shin, S.H., Lim, H.W., 2018. Changes in the optic nerve head induced by horizontal eye movements. PLOS ONE 13 (9), e0204069. https://doi.org/10.1371/journal.pone.0204069.

McGovern, R.A., Moosa, N.V., Jehi, A., Busch, L., Ferguson, R., Gupta, L., Gonzalez-Martinez, A., Wyllie, J., Najm, E., I, Bingaman, W.E., 2019. Hemispherectomy in adults and adolescents: Seizure and functional outcomes in 47 patients. Epilepsia 60 (12), 2416–2427. https://doi.org/10.1111/epi.16378.

Mehta, J.S., Plant, G.T., 2005. Optical Coherence Tomography (OCT) Findings in Congenital/Long-Standing Homonymous Hemianopia. Am. J. Ophthalmol. 140 (4), 727–729. https://doi.org/10.1016/j.ajo.2005.03.059.

Millington, R.S., Yasuda, C.L., Jindahra, P., Jenkinson, M., Barbur, J.L., Kennard, C., Cendes, F., Plant, G.T., Bridge, H., 2014. Quantifying the pattern of optic tract degeneration in human hemianopia. J. Neurol., Neurosurg. Psychiatry 85 (4), 379–386. https://doi.org/10.1136/jnnp-2013-306577.

Moosa, A.N.V., Jehi, L., Marashly, A., Cosmo, G., Lachhwani, D., Wyllie, E., Kotagal, P., Bingaman, W., Gupta, A., 2013. Long-term functional outcomes and their predictors after hemispherectomy in 115 children. Epilepsia 54 (10), 1771–1779. https://doi.org/10.1111/epi.12342.

Muckli, L., Naumer, M.J., Singer, W., 2009. Bilateral visual field maps in a patient with only one hemisphere. Proc. Natl. Acad. Sci. 106 (31), 13034–13039. https://doi.org/10.1073/pnas.0809688106.

Ong, Y.-H., Brown, M.M., Robinson, P., Plant, G.T., Husain, M., Leff, A.P., 2012. Read-Right: a “web app” that improves reading speeds in patients with hemianopia. J. Neurol. 259 (12), 2611–2615. https://doi.org/10.1007/s00415-012-6549-8.

Ptito, A., Fortin, A., Ptito, M., 2001. ‘Seeing’ in the blind hemifield following hemispherectomy. Prog. Brain Res. 134, 367–378. https://doi.org/10.1016/S0079-6123(01)34024-4.

Pulsifer, M.B., Brandt, J., Salorio, C.F., Vining, E.P.G., Carson, B.S., Freeman, J.M., 2004. The Cognitive Outcome of Hemispherectomy in 71 Children. Epilepsia 45 (3), 243–254. https://doi.org/10.1111/j.0013-9580.2004.15303.x.

Rispoli, J., Seay, M., Sum, M., Rucker, J.C., Shepherd, T.M., 2019. Clinical and Diffusion Tensor MRI Findings in Congenital Homonymous Hemianopia. J. Neuro-Ophthalmol. 39 (3), 401–404. https://doi.org/10.1097/WNO.0000000000000770.

Roebroeck, A., Galuske, R., Formisano, E., Chiry, O., Bratzke, H., Ronen, I., Kim, D., Goebel, R., 2008. High-resolution diffusion tensor imaging and tractography of the human optic chiasm at 9.4 T. NeuroImage 39 (1), 157–168. https://doi.org/10.1016/j.neuroimage.2007.08.015.

Sarlls, J.E., Pierpaoli, C., 2009. In vivo diffusion tensor imaging of the human optic chiasm at sub-millimeter resolution. NeuroImage 47 (4), 1244–1251. https://doi.org/10.1016/j.neuroimage.2009.05.098.

Sengupta, S., Smith, D.S., Smith, A.K., Welch, E.B., Smith, S.A., 2017. Dynamic Imaging of the Eye, Optic Nerve, and Extraocular Muscles With Golden Angle Radial MRI. Investig. Opthalmol. Visual Sci. 58 (10), 4390. https://doi.org/10.1167/iovs.17-21861.

Smith, S.A., Williams, Z.R., Ratchford, J.N., Newsome, S.D., Farrell, S.K., Farrell, J.A.D., Gifford, A., Miller, N.R., van Zijl, P.C.M., Calabresi, P.A., Reich, D.S., 2011. Diffusion tensor imaging of the optic nerve in multiple sclerosis: association with retinal damage and visual disability. Am. J. Neuroradiol. 32 (9), 1662–1668. https://doi.org/10.3174/ajnr.A2574.

Tournier, J.-D., Calamante, F., Connelly, A., 2012. MRtrix: diffusion tractography in crossing fiber regions. Int. J. Imaging Syst. Technol. 22 (1), 53–66. https://doi.org/10.1002/ima.22005.

Tournier, J.-D., Smith, R., Raffelt, D., Tabbara, R., Dhollander, T., Pietsch, M., Christiaens, D., Jeurissen, B., Yeh, C.-H., Connelly, A., 2019. MRtrix3: A fast, flexible and open software framework for medical image processing and visualisation. NeuroImage 202, 116137. https://doi.org/10.1016/j.neuroimage.2019.116137.

Traub-Weidinger, T., Weidinger, P., Gröppel, G., Karanikas, G., Wadsak, W., Kasprian, G., Dorfer, C., Dressler, A., Muehlebner, A., Hacker, M., Czech, T., Feucht, M., 2016. Presurgical evaluation of pediatric epilepsy patients prior to hemispherotomy: the prognostic value of 18F-FDG PET. J. Neurosurg.: Pediatr. 18 (6), 683–688. https://doi.org/10.3171/2016.5.PEDS1652.

Trip, S.A., Schlottmann, P.G., Jones, S.J., Li, W.-Y., Garway-Heath, D.F., Thompson, A.J., Plant, G.T., Miller, D.H., 2006. Optic nerve atrophy and retinal nerve fibre layer thinning following optic neuritis: Evidence that axonal loss is a substrate of MRI-detected atrophy. NeuroImage 31 (1), 286–293. https://doi.org/10.1016/j.neuroimage.2005.11.051.

Vargha-Khadem, F., 1997. Onset of speech after left hemispherectomy in a nine-year-old boy. Brain 120 (1), 159–182. https://doi.org/10.1093/brain/120.1.159.

Veraart, J., Novikov, D.S., Christiaens, D., Ades-aron, B., Sijbers, J., Fieremans, E., 2016. Denoising of diffusion MRI using random matrix theory. NeuroImage 142, 394–406. https://doi.org/10.1016/j.neuroimage.2016.08.016.

Waddington, J., Linehan, C., Gerling, K., Williams, C., Robson, L., Ellis, R., Hodgson, T., 2018. Evaluation of eyelander, a video game designed to engage children and young people with homonymous visual field loss in compensatory training. J. Visual Impair. Blind. 112 (6), 717–730. https://doi.org/10.1177/0145482X1811200607.

Werth, R., 2006. Visual functions without the occipital lobe or after cerebral hemispherectomy in infancy. Eur. J. Neurosci. 24 (10), 2932–2944. https://doi.org/10.1111/j.1460-9568.2006.05171.x.

Winston, G.P., Daga, P., White, M.J., Micallef, C., Miserocchi, A., Mancini, L., Modat, M., Stretton, J., Sidhu, M.K., Symms, M.R., Lythgoe, D.J., Thornton, J., Yousry, T.A., Ourselin, S., Duncan, J.S., McEvoy, A.W., 2014. Preventing visual field deficits from neurosurgery. Neurology 83 (7), 604–611. https://doi.org/10.1212/WNL.0000000000000685.